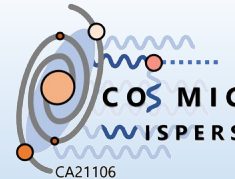


Searching for a new light boson with PADME

Kalina Dimitrova
Faculty of Physics, Sofia University
kalina@phys.uni-sofia.bg

LA THUILE 2026 - Les Rencontres de Physique de la Vallée d'Aoste
Mar 01 – 07, 2026
La Thuile, Italy



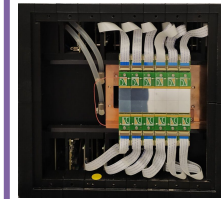
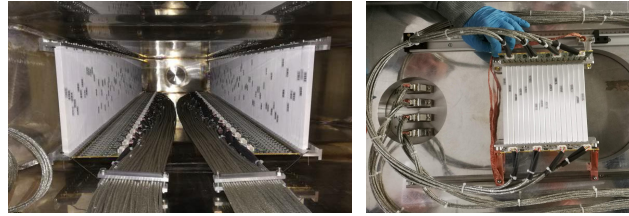
* partially supported by BNSF KP-06-COST/25 from
16.12.2024, COST Action COSMIC WISPERs CA21106

The PADME Experiment



Charged particle veto system

96 + 96 (90) + 16 (x2) plastic scintillator-WLS-SiPM RO channels
Segmentation provides momentum measurement down to ~ 5 MeV resolution

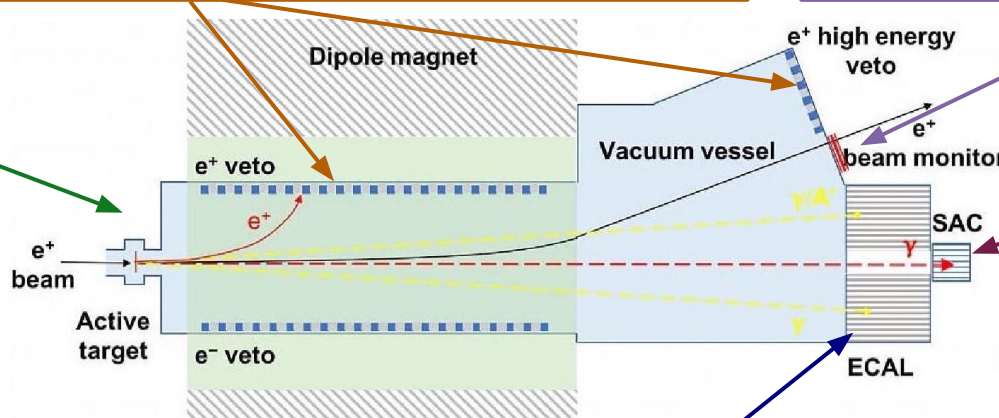
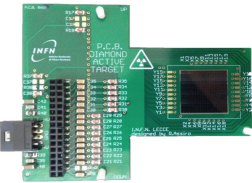


TimePix3 beam monitor at beam exit window

Matrix of 2 x 6 detectors for a total of 1536 x 512 pixels

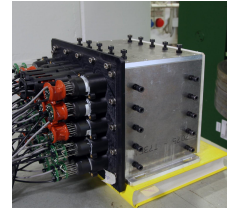
Active diamond target

2 x 16 graphite electrodes: XY beam profile and multiplicity



Small-angle calorimeter (SAC)

25 crystals - 5 x 5 matrix, Cherenkov PbF_2

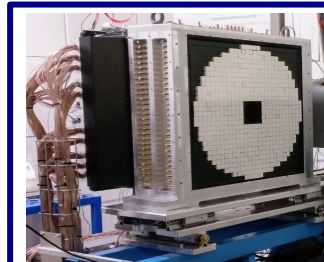


Dipole magnet



Electromagnetic calorimeter (ECAL)

616 BGO crystals, $2.1 \times 2.1 \times 23 \text{ cm}^3$
BGO covered with diffuse reflective TiO_2 paint; additional optical isolation: 50 – 100 μm black tedlar foils
Scintillation light decay time – $O(300 \text{ ns})$

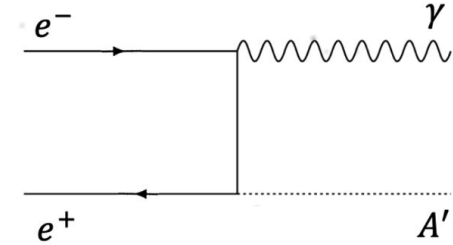
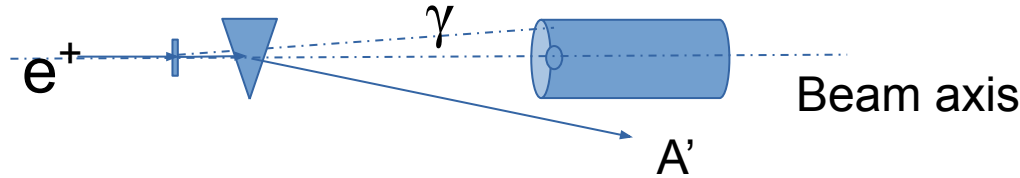


PADME Run II Dark Photon search



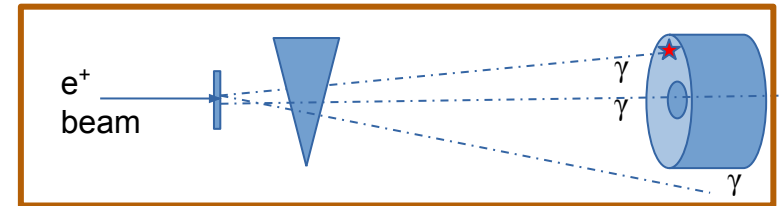
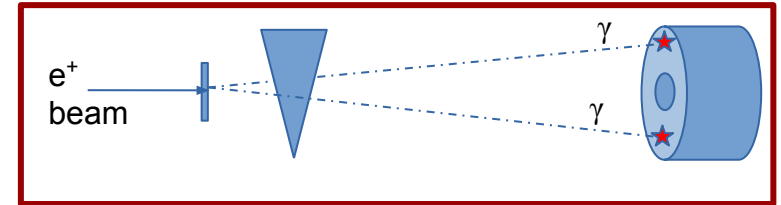
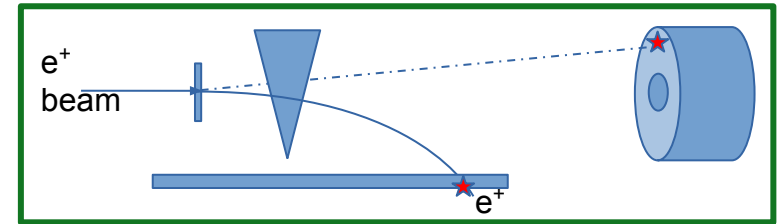
Associated production: $e^+ e^- \rightarrow A' \gamma$
 Search for single photon events and calculate the missing mass

$$M_{\text{miss}}^2 = (p_{\text{pos}} + p_{\text{elec}} - p_{\gamma})^2$$



Background composition:

- **Bremsstrahlung in the field of the target nuclei:** Photons mostly @ low energy, background dominates the high missing masses
- **2 photon annihilation:** Peaks at $M_{\text{miss}} = 0$
- **3 photon annihilation:** symmetry is lost – decrease in the vetoing capabilities
- **Radiative Bhabha scattering**

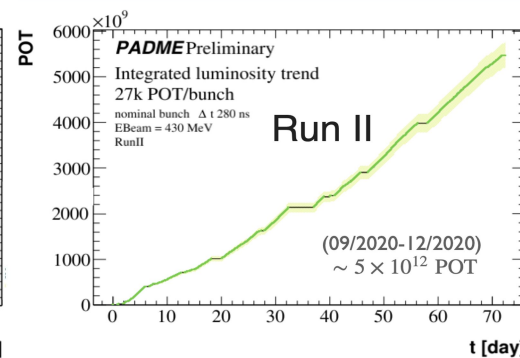
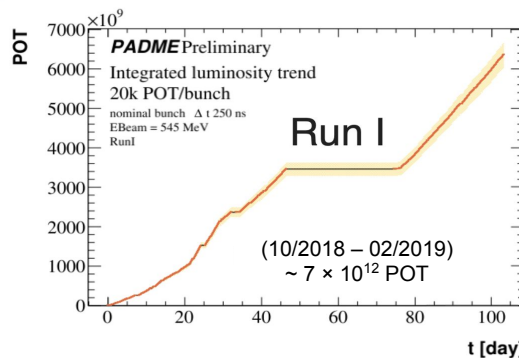


Run II data taking and results



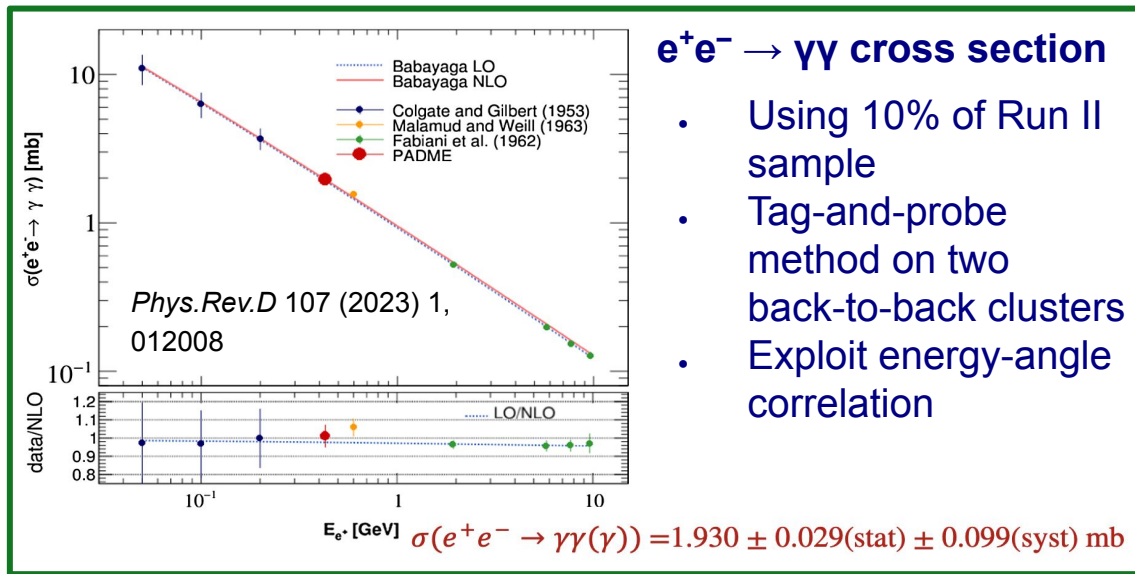
Run I and PADME commissioning

- Started in Autumn 2018 and ended on February 25th
 - $\sim 7 \times 10^{12}$ PoT recorded with secondary beam
 - PADME DAQ, Detector, beam, collaboration commissioning
 - Data quality and detector calibration
- PADME test beam data
 - July 2019, few days of valuable data: certification of the primary beam
 - Detector performance/calibration checks
 - Primary beam with $E_{\text{beam}} = 490$ MeV



Run II: primary beam

- July 2020
 - New environment/detector parameter monitoring and control system
 - Remote operation confirmation
- Autumn 2020:
 - A long data taking period with $O(5 \times 10^{12})$ e^+ on target
 - $E_{\text{beam}} = 430$ MeV



$e^+e^- \rightarrow \gamma\gamma$ cross section

- Using 10% of Run II sample
- Tag-and-probe method on two back-to-back clusters
- Exploit energy-angle correlation

$$E_0 [\text{GeV}] \quad \sigma(e^+e^- \rightarrow \gamma\gamma(\gamma)) = 1.930 \pm 0.029(\text{stat}) \pm 0.099(\text{syst}) \text{ mb}$$

Run II Dark Photon Analysis



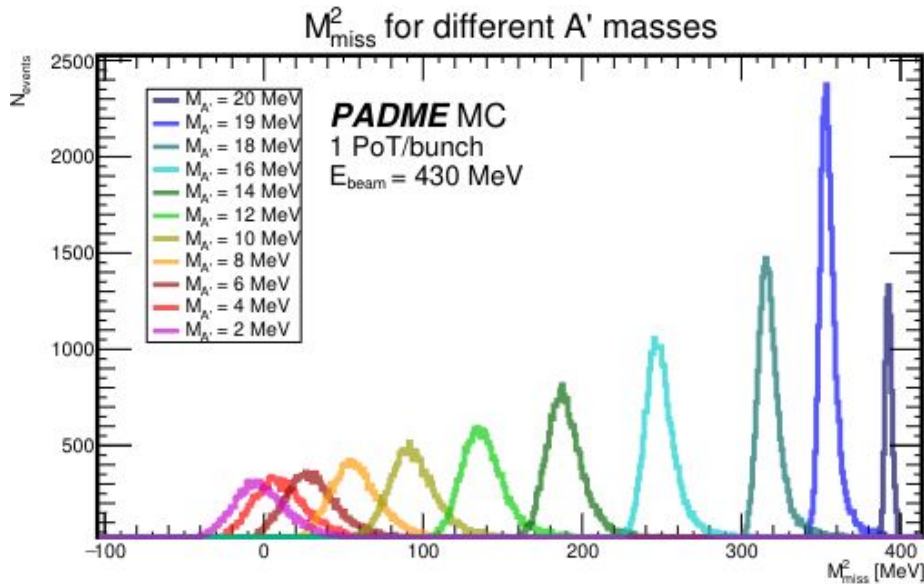
$$N_{A'} = N_{pots} \sigma(\epsilon) \frac{\rho d \mathcal{N}_A Z}{M}$$

5×10^{12}
for Run II

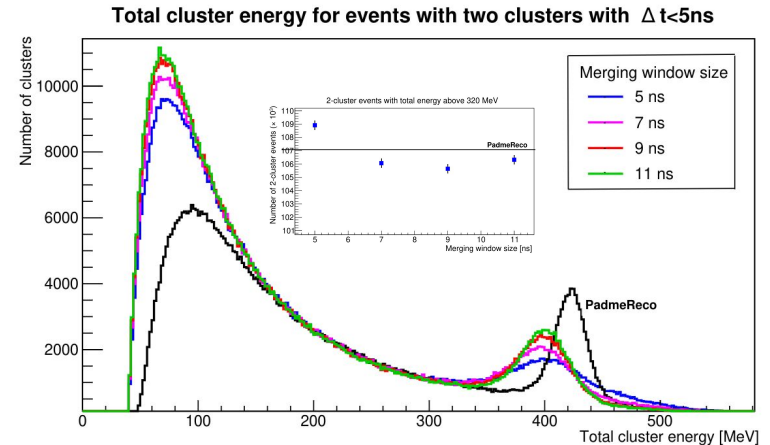
0.0106/barn
(number of e^- /unit of
area of the target)

Check obtained cross-section
values using $\gamma\gamma$ result

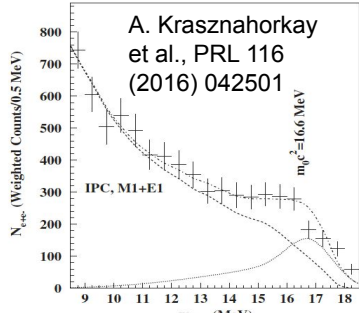
$$\frac{\sigma(e^+e^- \rightarrow U\gamma)}{\sigma(e^+e^- \rightarrow \gamma\gamma)} = \epsilon^2 * \delta$$



Machine learning models were tested for the reconstruction of $e^+e^- \rightarrow \gamma\gamma$ events in Run II data and compared to the conventional reconstruction

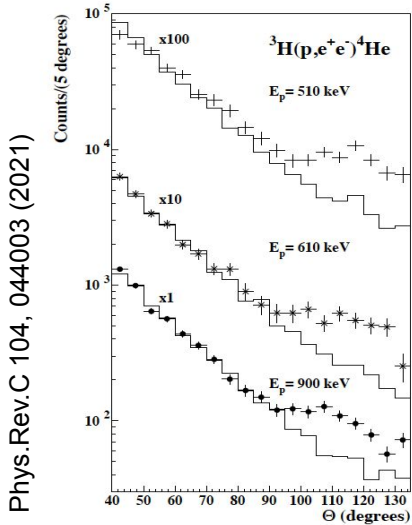
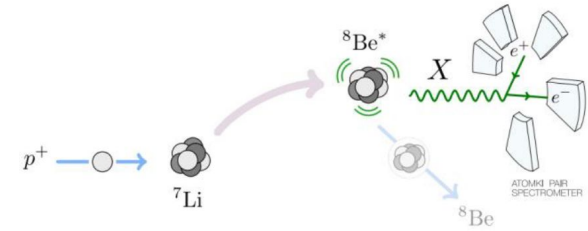


The X17 anomaly

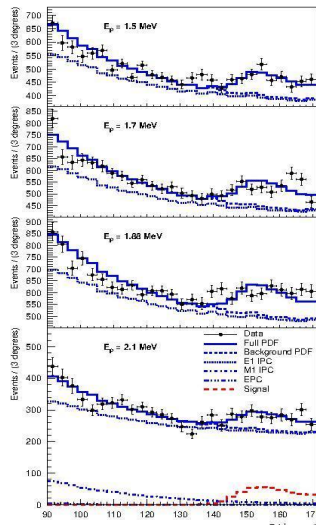


Excess in e^+e^- pairs angular correlation:

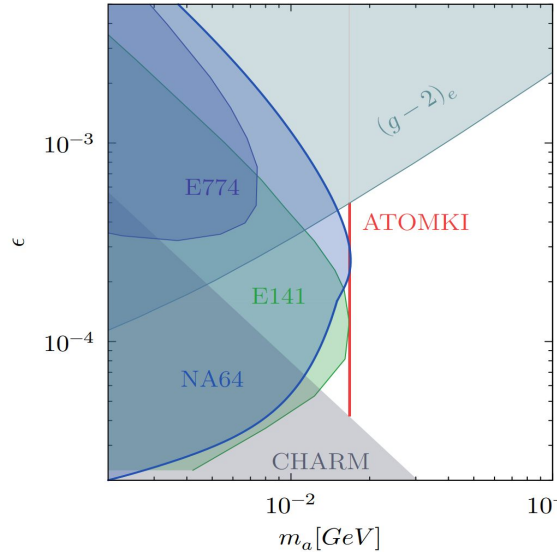
- Similar physics observables in ^8Be , ^4He and ^{12}C experiments: 2 leptons in the final state, produced via internal pair conversion
- Kinematics properties determined by the mass of a decaying X particle, compatible with $M_X \sim 17$ MeV



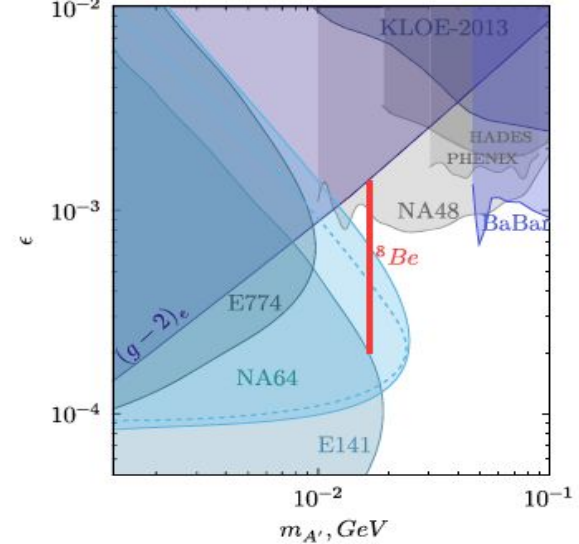
Phys. Rev. C 106, L061601 (2022)



Phys. Rev. D 101, 071101(R) (2020)



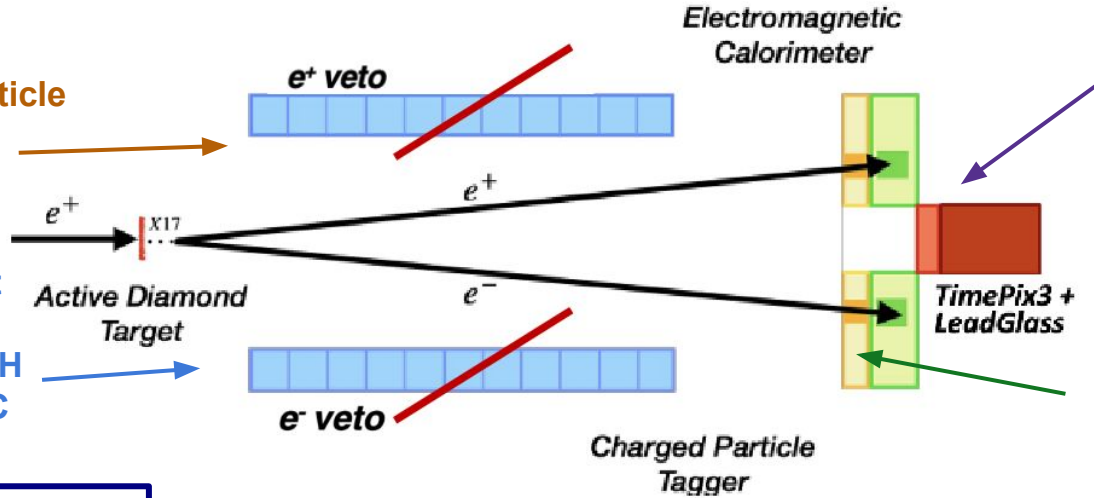
Phys. Rev. D 104, L111102 (2021)



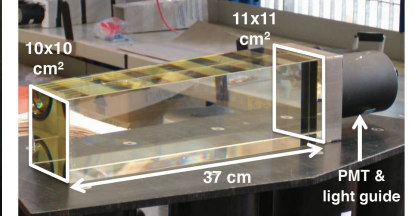
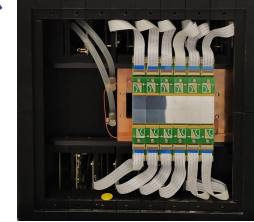
PADME X17 Search

Charged particle veto system switched off

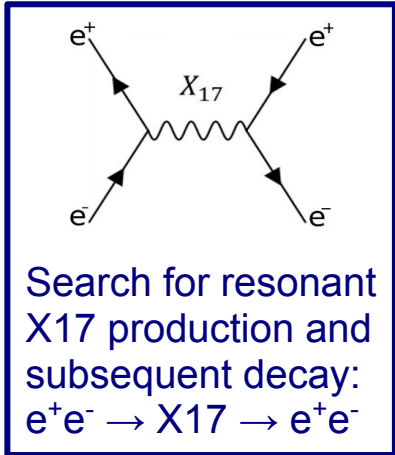
Dipole magnet switched off: **RUNNING WITH NO MAGNETIC FIELD**



SAC replaced with TimePix3 + Lead Glass beam monitoring system



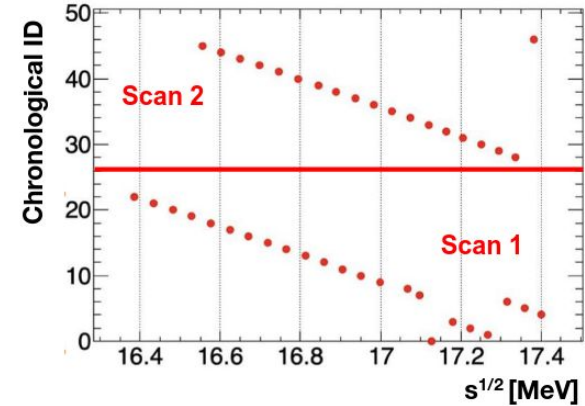
Charged particle tagger (ETag) placed in front of the ECal (plastic scintillator array)



Goal: measure the e^+e^- final state and look for excess above the SM background

Data-taking divided in 3 parts:

- Nominal scan: 47 points (scan 1 and 2) @ (263-299) MeV, corresponding to $\sqrt{s} = [16.4, 17.4]$ MeV
- Below resonance: 5 points @ (205-211) MeV
- Above resonance: 5 points @ 402.5 MeV



Run III analysis strategy

Main analysis observable: the ratio $g_R(s)$ between the number of observed events with a two-body final state and the expected number of background events

$$g_R(s) = \frac{N_2(s)}{N_{POT}(s) \cdot B(s)} = \begin{cases} K(s) \left[1 + \frac{S(s; M_X, g_{V_e}) \cdot \epsilon_{sig}(s)}{B(s)} \right] & \text{Signal + background hypothesis} \\ K(s) & \text{Background-only hypothesis} \end{cases}$$

$N_2(S)$ - number of two-cluster events selected

$N_{POT}(S)$ - number of positrons on target

$B(S)$ - expected background yield per POT

$S(s; M_X, g_{V_e})$ - expected signal production for mass M_X and coupling g_{V_e}

$\epsilon_{sig}(s)$ - signal acceptance and selection efficiency

$K(s)$ - DATA-MC scale factor with a possible additional linear dependence on \sqrt{s}

Goal: measure the two-body final state and evaluate systematic errors. Establish if the obtained rate is compatible with SM expectation or with the presence of an hypothetical X17 signal

N₂ selection

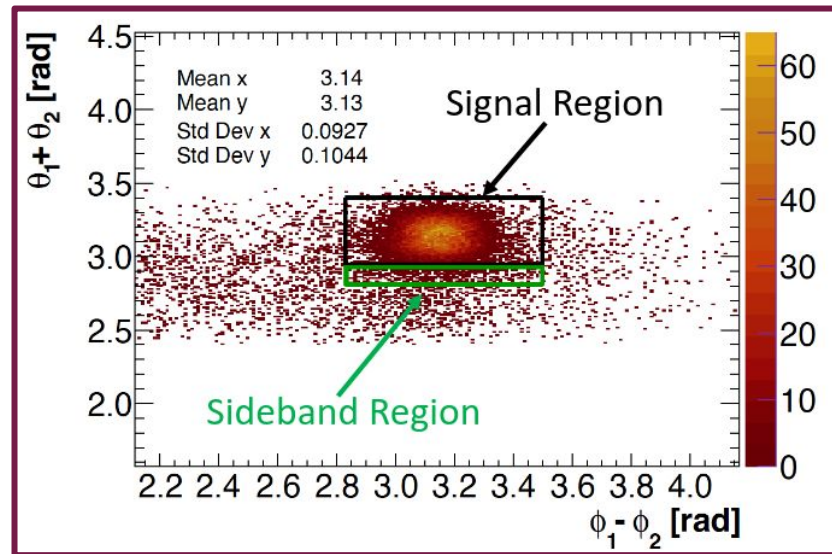
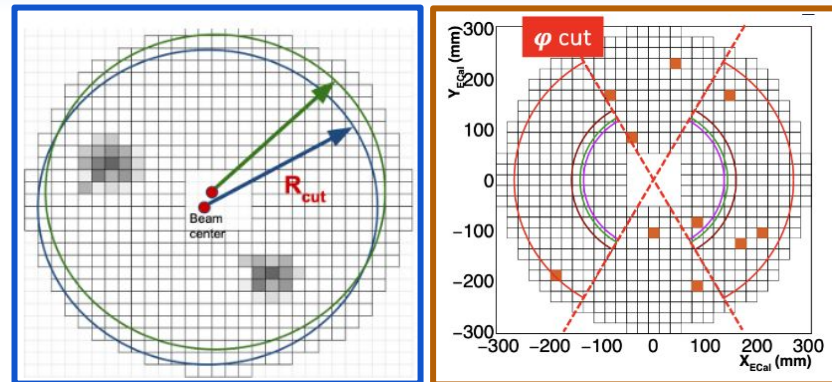
Selection of two-cluster events in the ECal - algorithm as independent as possible on beam and detector conditions:

- Maximum radius defined by ECAL dimensions
- Minimum radius within the “two-cluster” kinematic range → following the beam center conditions
- Energy within the “two-cluster” kinematic range
- ECAL illumination affected by material along the beam line (below flange) → Cut regions in φ

Two cluster selection cuts:

- Time difference $\Delta T < 5$ ns
- Distance $\Delta R > 60$ mm (minimum GG difference)
- $\phi_1 - \phi_2$ vs $\theta_1 + \theta_2$ cut in the center of mass frame isolates the signal

Source	Error on N ₂ [%]
Statistics	~ 0.6
Background subtraction	0.3
Total	0.65



N_{PoT} estimation



PoTs measured with the end-of-line lead glass calorimeter:

$$N_{PoT} = \frac{Q_{LG}}{Q_{1e^+,402[MeV]}} \times \frac{402}{E_{beam}[MeV]}$$

Uncorrelated systematic errors

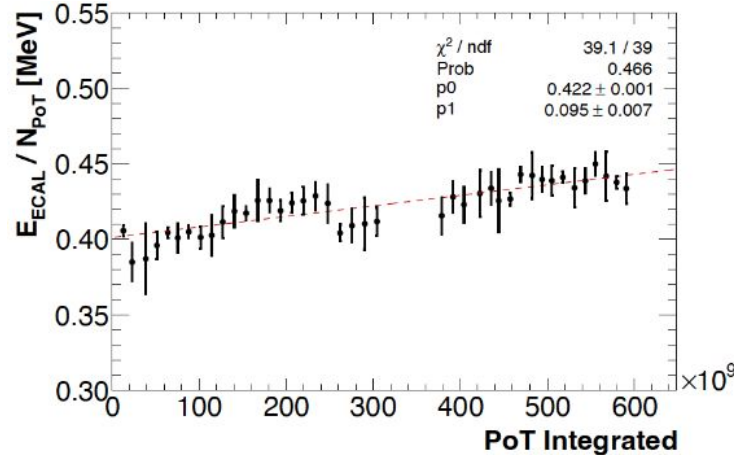
Source	Error on N_{PoT} [%]
Statistics, ped subtraction	negligible
Energy scale from BES	0.3
Rad. induced loss, slope	Variable, ~0.35
Total	0.45

Common systematic errors

Source	Common error [%]
pC / MeV (JHEP 08 (2024) 121)	2.0
Energy Loss, data/MC	0.5
Rad. induced loss	0.3
Total	2.1

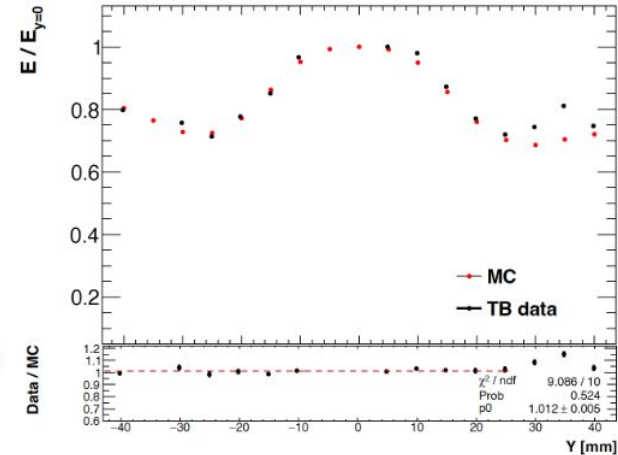
Radiation induced loss

- Run III dose ~ 2.5 krad → transparency changes for O(krad)
- Linear energy dependence on the integrated flux → LG yield decreases by 0.097 ± 0.007 → NPoT flux corrected
- Error associated both to the constant term and to the slope of the correction



Energy loss in passive material

- Beam movements → passive material crossing (TimePix cooling system)
- Test beam: evaluate the overall energy loss for the specific beam conditions → flux corrected for each energy point

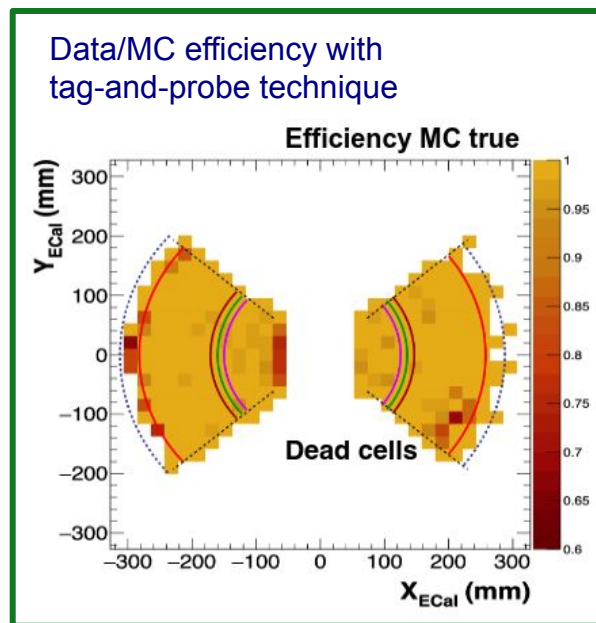


Expected background B(s)

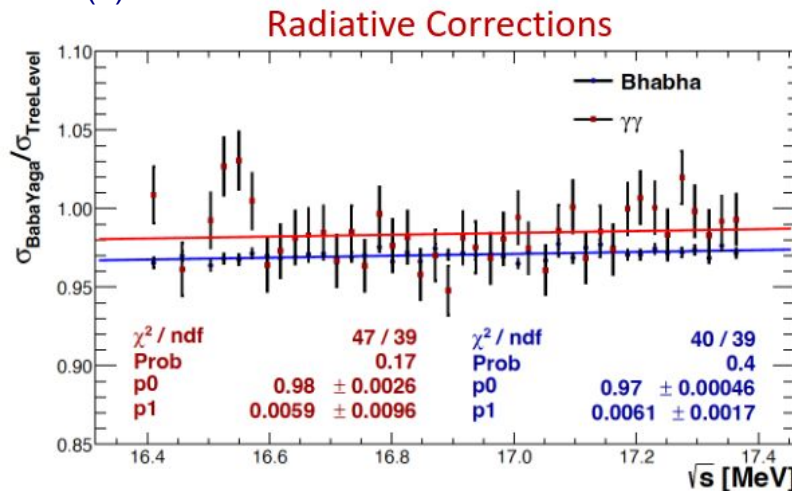
The expected background / e⁺, B(s), is determined with MC and validated with data-driven checks.

- Reconstruction efficiency estimated with Tag&Probe method
- Background subtraction at tag level dominates the statistical-systematic error → $\delta B = 0.35\%$
- Beam spot direction & shape → acceptance variation of 0.08% - 0.1% / mm of vertical shift
- Stability of cuts due to acceptance edge effects and leakage → estimated by varying R_{\max}

Source of uncertainty	Error on B [%]
MC statistics	0.40
Data/MC efficiency (Tag&Probe)	0.35
Cut stability	0.04
Beam spot variations	0.05
Total	0.54



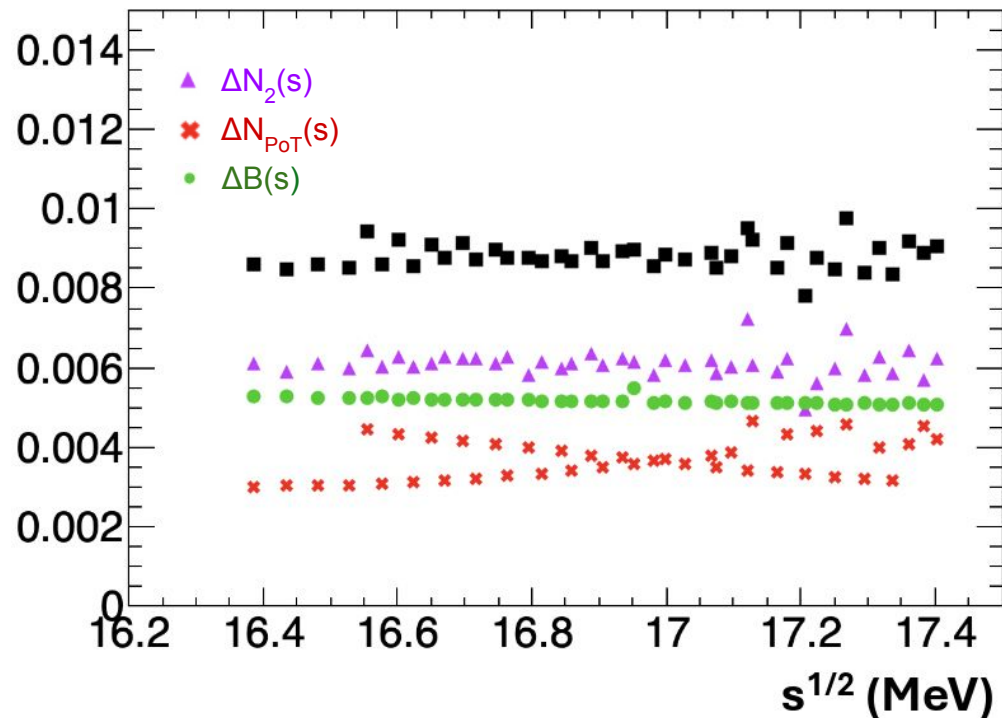
Radiative corrections e⁺e⁻(γ) and $\gamma\gamma(\gamma)$ evaluated using BabaYaga → 3% decrease in the total cross section @ 16.92 MeV and a \sqrt{s} slope of -0.6(6) % MeV⁻¹



Total error budget

Uncorrelated uncertainty on $g_R(s) = N_2(s) / (N_{PoT}(s) B(s))$:

Relative uncorrelated error per period



Next step: is $g_R(s)$ compatible with 1 or $1 + (S(s) \epsilon(s) / B(s))$?

Uncorrelated errors

Source	Uncertainty (% per energy point)
$N_2(s)$	0.60
$B(s)$	0.54
$N_{PoT}(s)$	0.35
Total on $g_R(s)$	0.88

$K(s)$, constant term

Source	Uncertainty (%)
Lead-glass calibration	2.0
Absolute B yield	1.8
Energy-loss correction to N_{PoT}	0.5
Radiation-induced correction to N_{PoT}	0.3
Total	2.8

$K(s)$, \sqrt{s} -slope

Source	Expected value (%/MeV)
Radiative corrections	$-0.6 \pm 0.2 \pm 0.6$
Total	-0.6 ± 0.6

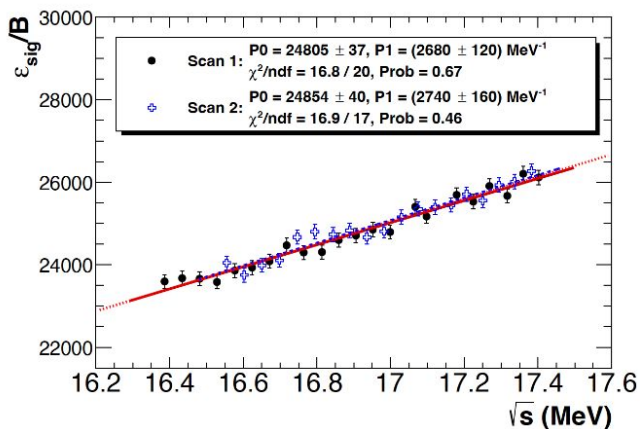
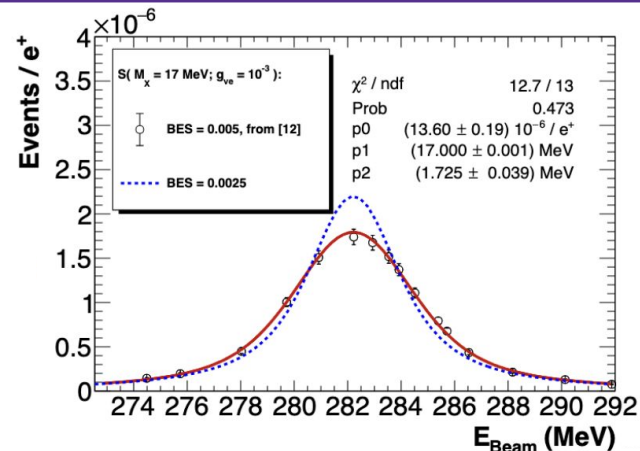
Signal yield $S(s; M, g_\nu)$ and efficiency $\varepsilon_{\text{sig}}/B$

Signal yield: the width of the expected excess depends on the beam energy spread (BES) the electron motion in the target.

Functional form is a Voigt distribution parametrized as function of the beam energy: **convolution of the Gaussian for the BES with a Lorentzian** →

Uncertainty in the curve parameters as nuisances:

- Lorentzian width around the resonance energy: 1.72(4) MeV
- Relative BES: 0.025(5)%



Expected signal efficiency determined from MC:

Use of the ratio $\varepsilon_{\text{sig}}/B$ significantly reduces detector-related systematic uncertainties (similar detector illumination for both signal and background).

→ Fit $\varepsilon_{\text{sig}}/B$ with a straight line → fit parameters as nuisances:

- Errors: $\Delta P0/P0 \sim 0.1\%$, $\Delta P1/P1 = 3\%$, correlation = -1.8



Blind - unblinding procedure

Large expected X17 mass resolution \rightarrow no sideband region in \sqrt{s} can be defined to validate the statistical approach \rightarrow Validation procedure described in *JHEP 06 (2025) 040* was used

- Aim to blindly define a sideband in $g_R(s)$, excluding 10 periods of the scan
- Define the masked periods by optimizing the probability of a linear fit in s
- Data validation criteria are based on the fit quality, the distribution of the fit pulls, and the parameters of the linear fit

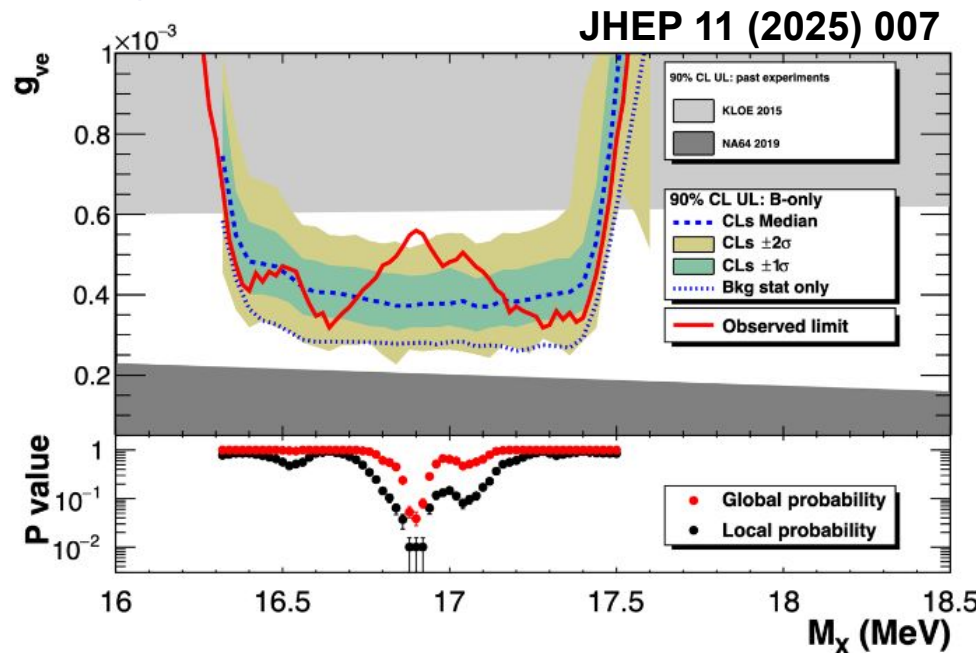
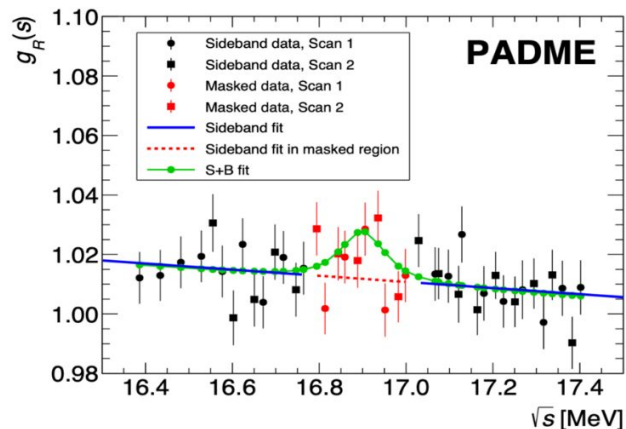
Statistical treatment

Test statistic based on likelihood ratio between S+B and B-only and includes terms for each nuisance parameter

Upper limit on g_{ve} defined as $CL_S = \frac{P_S}{(1 - P_B)}$ for a given M_x

Results

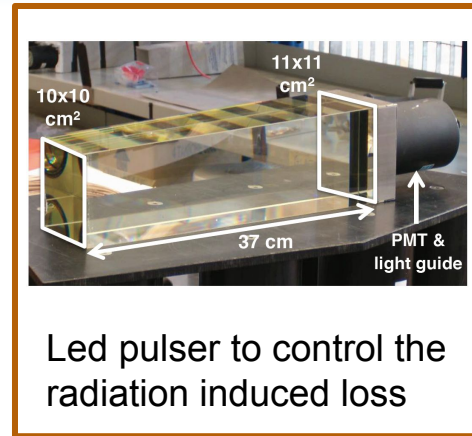
- The observed limit is consistent with the expected for most of the parameter space
- Slight excess observed, 2.5σ local, $1.8(2) \sigma$ global significance corresponding to mass $M_x = 16.9 \text{ MeV}$ and a coupling $g_{ve} = 5 \times 10^{-4}$



PADME Run IV improvements

PADME Run IV realized in 2025: optimized setup with increased sensibility to confirm/disprove Run III result

- **Diamond target moved downstream by ~30 cm**
- Passive material removed and PADME Magnet fully degaussed → $B < 1$ G
- Beam stable in the central position along the whole data taking → NO LATERAL LEAKAGE on the beam catcher
- **Led pulser Tektronix AFG3101 to control the radiation induced loss**
 - Independent trigger included in the DAQ
 - A second LG block installed (out of the acceptance and only acquiring the LED trigger)
 - Online LG response renormalized to the not-fired-block
 - Almost instant reference for light yield response



Source	Uncertainty [%]		Improvement
	Run III	Run IV	
N_2	0.6	0.3	New target position → acceptance increased
B	0.35	0.3	PadMME → ee/ $\gamma\gamma$ discrimination + better angular momentum resolution
N_{PoT}	0.55	0.3	Three different beam spot monitor (target-PadMME-TMM) + online LG calibration system
Total	0.88	0.5	

PADME Run IV improvements

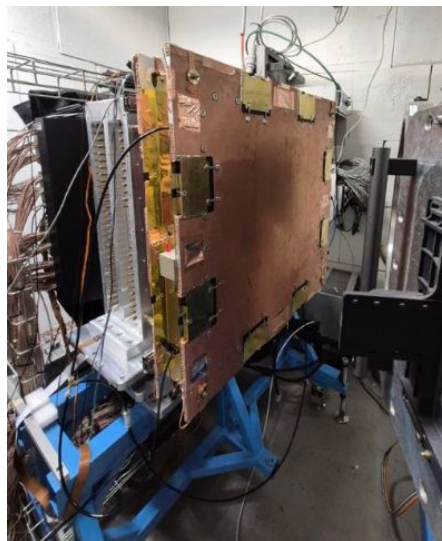
PadMMe MicroMegas chamber (replaced the Etagger):

- e/ γ discrimination \rightarrow possible normalization to $e^+e^- \rightarrow \gamma\gamma$ process
- Spatial resolution $\sim 350 \mu\text{m}$ \rightarrow angle disentanglement
- Multitrack events can be collected
- Beam spot monitor \rightarrow Implemented in the Run IV online monitor
- 3 HV regions for a better control on the amplification in the "beam" region
- Gas Mixture Ar:CF₄:Isobutane (88:10:2)

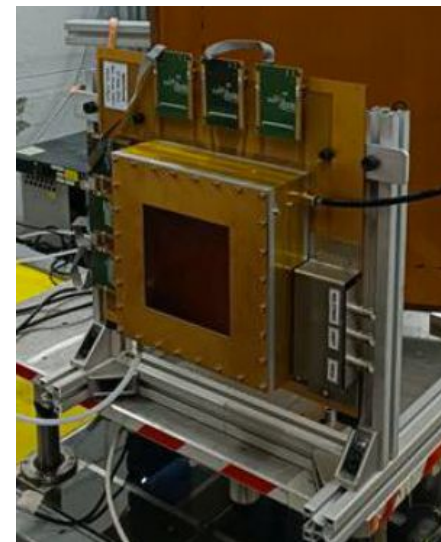
TMM MicroMegas (replaced the TimePix beam monitor)

- Greater active area wrt TimePix and less passive material budget
- Beam shape and spot monitor

PadMMe MicroMegas chamber



TMM MicroMegas



Conclusions

Run II

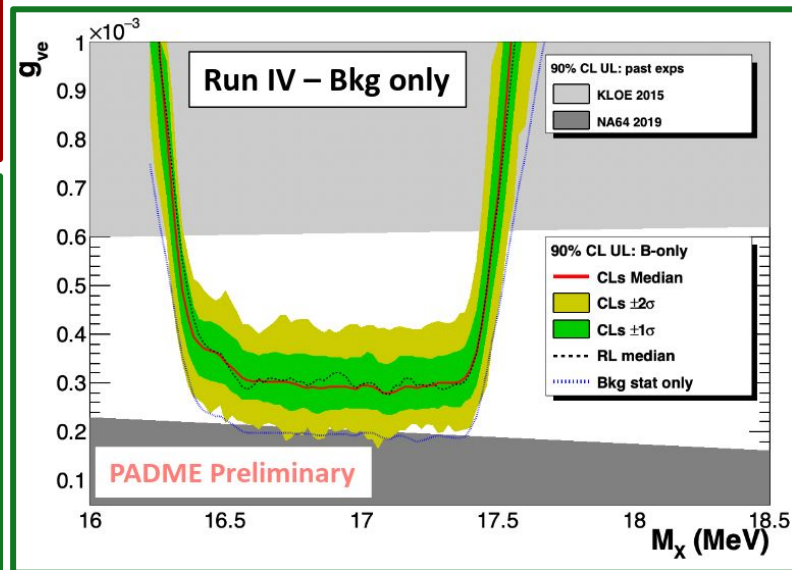
- About 5×10^{12} PoT with primary positron beam collected
- $e^+e^- \rightarrow \gamma\gamma$ cross section at $E_{e^+} = 430$ MeV measured with $\sim 5\%$ uncertainty
- Analysis for Dark Photon search currently ongoing

Run III

- Analysis has been completed: no indications of X17 well beyond two-sigma, slight excess has been observed at $M_X = 16.9$ MeV, with global p-value equivalent to $1.77(15)\sigma$

Run IV

- Improved setup: new Micromegas tracker installed to measure the absolute $ee/\gamma\gamma$ cross section + TMM to the end of the line for beam monitor
- Run IV-part 1 completed in July 2025
 - 18 energy scan points collected ($\sim 2 \times 10^{10}$ PoTs each) equally separated by 1.5 MeV in the range of $E_{\text{beam}} = (269.5, 295)$ MeV $\rightarrow \sqrt{s} = (16.60, 17.36)$ MeV
- Run IV-part 2 completed in November 2025
 - 18 scan points interspersing part 1 ones
 - Out-of-resonance: \sqrt{s} below 16 MeV and above 18 MeV



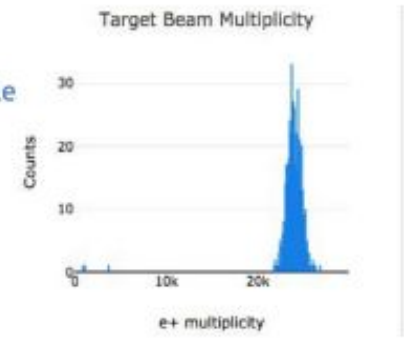
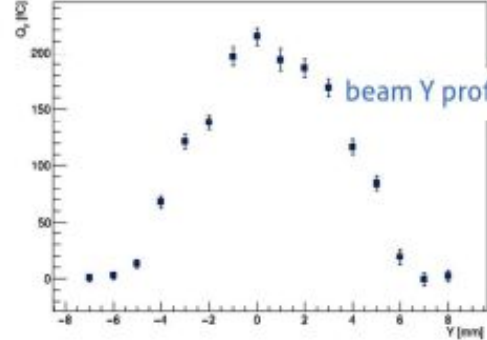
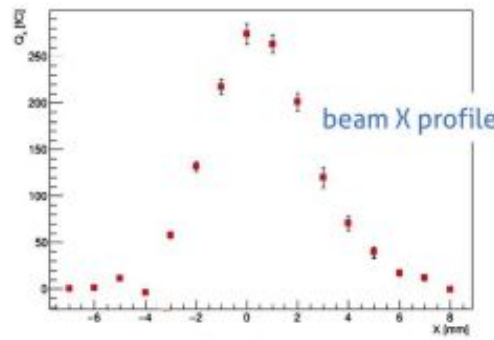
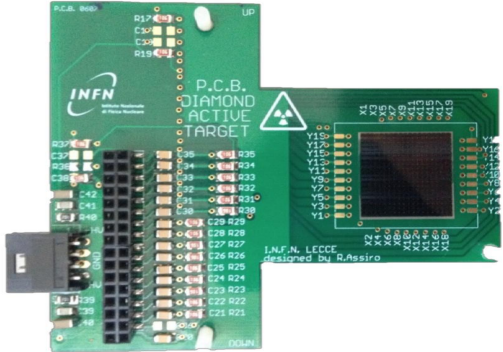
Backup slides



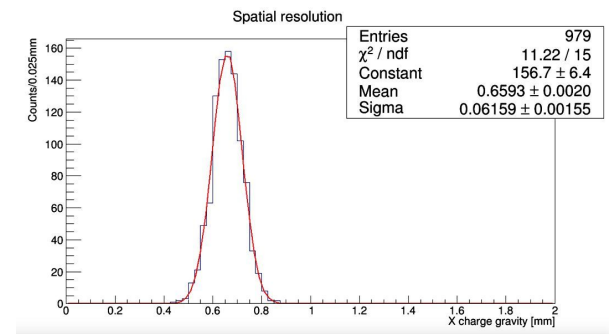
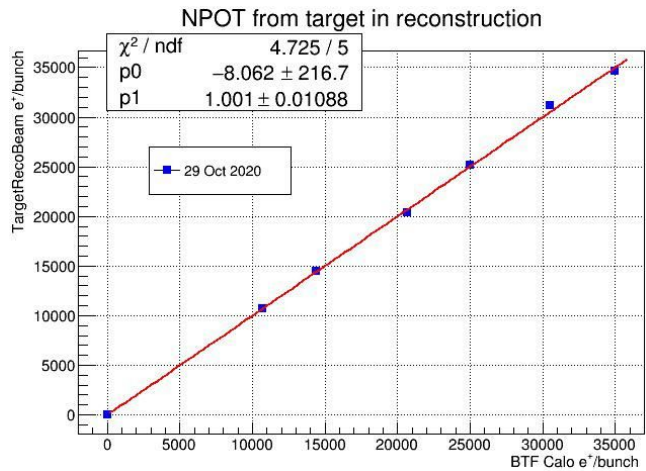
The PADME Experiment



Active target



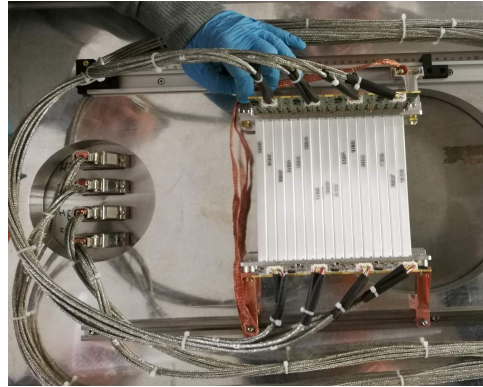
- Polycrystalline diamond:
 - 100 μm thickness:
 - $2 \times 16 \times 1$ mm strips provide X-Y readout in a single detector: graphite electrodes using excimer laser
 - Beam XY profile and multiplicity



JINST 12 (2017) 02, C02036

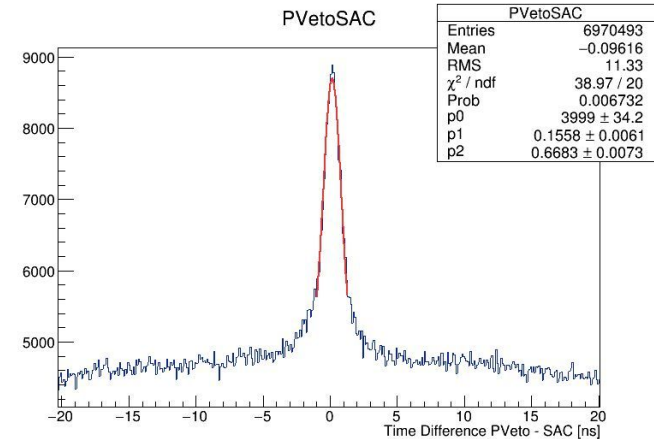
The PADME Experiment

Charged particle detectors



- Three sets of detectors detect the charged particles from the PADME target:
 - **PVeto**: positrons with $50 \text{ MeV} < p_{e^+} < 450 \text{ MeV}$
 - **HEPVeto**: positrons with $450 \text{ MeV} < p_{e^+} < 500 \text{ MeV}$
 - **EVeto**: electrons with $50 \text{ MeV} < p_{e^+} < 450 \text{ MeV}$
- 96 + 96 (90) + 16 (x2) plastic scintillator-WLS-SiPM RO channels
- Segmentation provides momentum measurement down to $\sim 5 \text{ MeV}$ resolution

- Custom SiPM electronics, Hamamatsu S13360 3 mm, 25 μm pixel SiPM
- Differential signals to the controllers, HV, thermal and current monitoring
- Online time resolution: $\sim 2 \text{ ns}$
- Offline time resolution after fine T_0 calculation – better than 1 ns

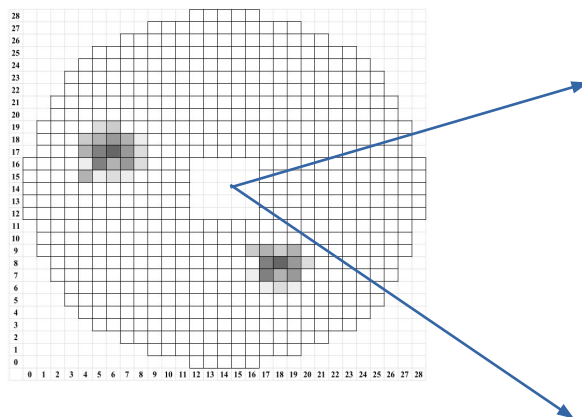
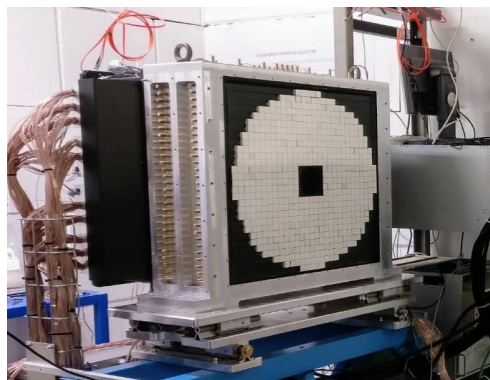


Time calibration with SAC using Bremsstrahlung events

The PADME Experiment

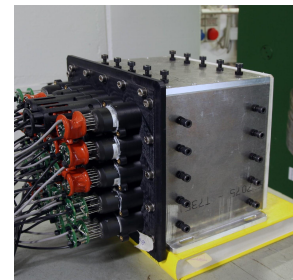


Electromagnetic calorimeter (ECal)



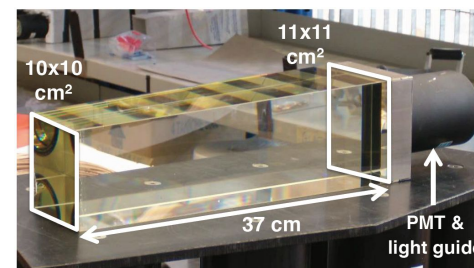
- 616 BGO crystals, $2.1 \times 2.1 \times 23 \text{ cm}^3$
- BGO covered with diffuse reflective TiO_2 paint
 - additional optical isolation: 50 – 100 μm black tedlar foils
- Scintillation light decay time – $O(300 \text{ ns})$

Run I and II: Small-angle calorimeter (SAC)



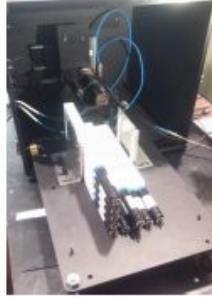
- 25 crystals - 5 x 5 matrix, Cherenkov PbF_2
- Time resolution: $< 100 \text{ ps}$
- Angular acceptance: $[0, 19] \text{ mrad}$

Run III: Beam monitoring system: TimePix3 + Lead Glass Calorimeter



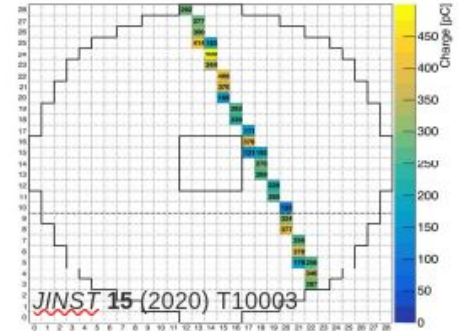
The PADME Experiment

PADME



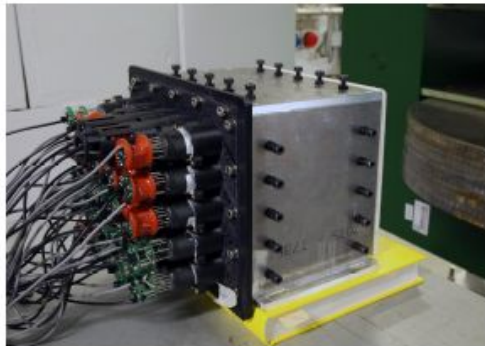
ECAL: The heart of PADME

- 616 BGO crystals, $2.1 \times 2.1 \times 23 \text{ cm}^3$
- BGO covered with diffuse reflective TiO_2 paint
- additional optical isolation: 50 – 100 μm black tedlar foils



Calibration at several stages:

- BGO + PMT equalization with ^{22}Na source before construction
- Cosmic rays calibration using the MPV of the spectrum
- Temperature monitoring

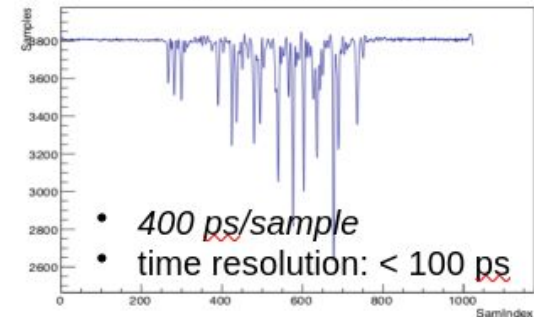


Small Angle Calorimeter (SAC)

- 25 crystals - 5 x 5 matrix, Cherenkov PbF_2
- Dimensions of each crystal: $3 \times 3 \times 14 \text{ cm}^3$
- 50 cm behind ECAL
- PMT readout: Hamamatsu R13478UV with custom dividers
- Angular acceptance: $[0,19] \text{ mrad}$

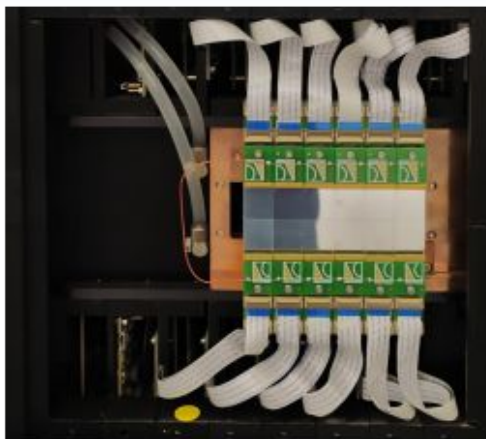
Nucl.Instrum.Meth.A 919 (2019) 89-97

Recorded bunch

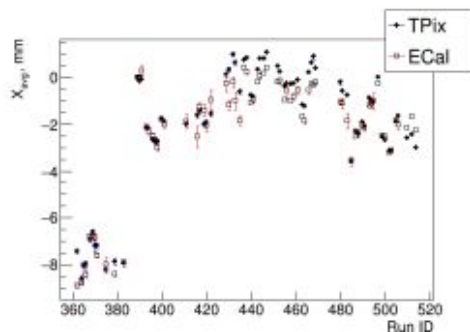


- 400 ps/sample
- time resolution: < 100 ps

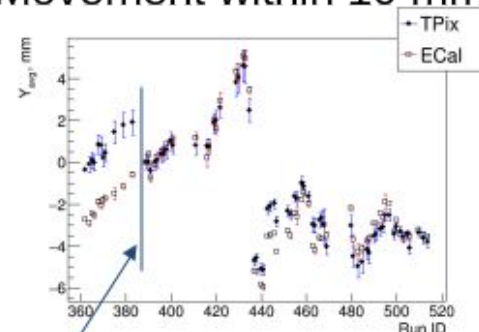
TimePix3 beam monitor



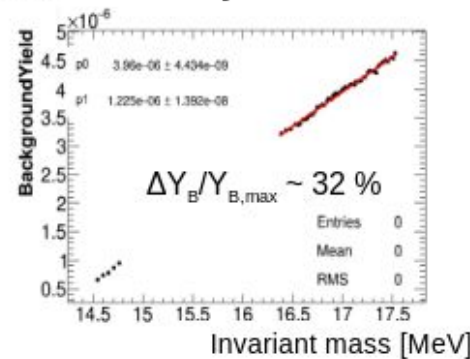
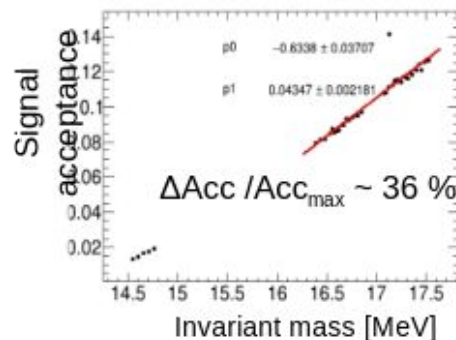
COG at the ECal front face from 2 cluster events



Movement within 10 mm

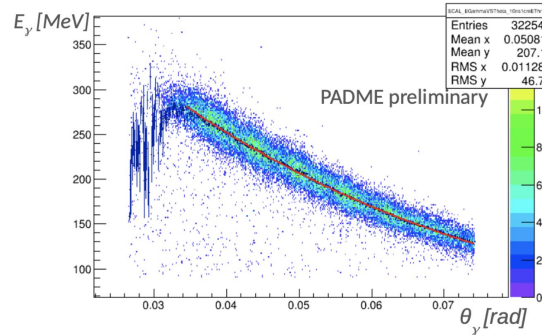
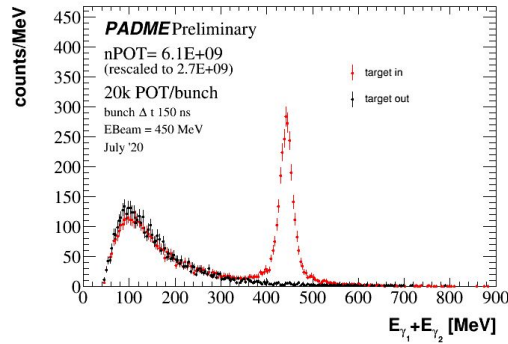


Timepix was moved by 1.8 mm



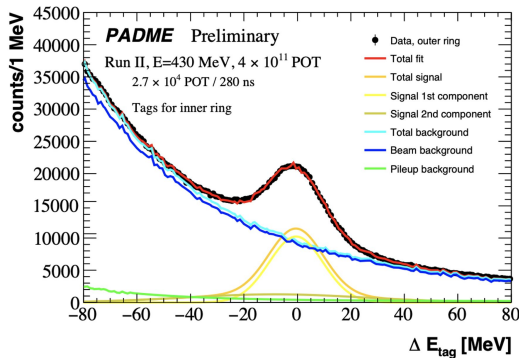
- Matrix of 2 x 6 Timepix3 detectors
 - each 256x256 pixels
- Operated in 2 modes:
 - image mode, integrating
 - streaming mode, feeding ToT and ToA for each fired pixel

$e^+e^- \rightarrow \gamma\gamma$ cross-section

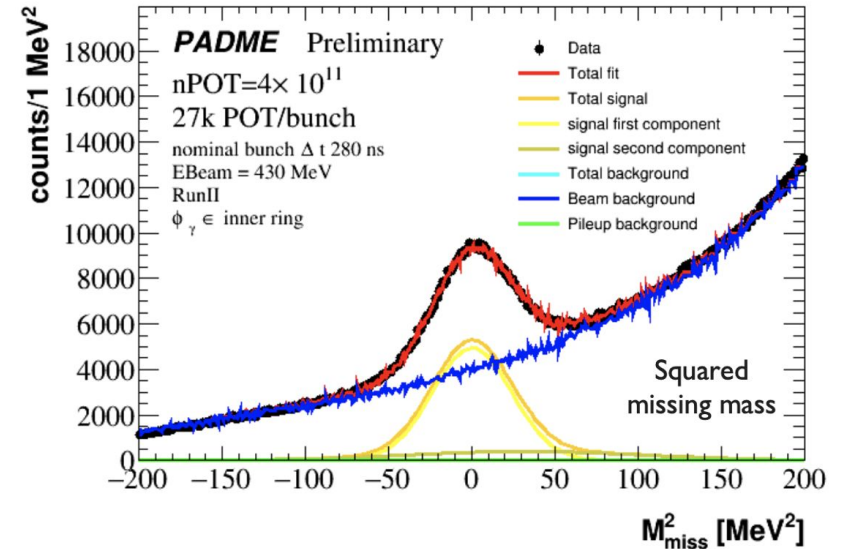
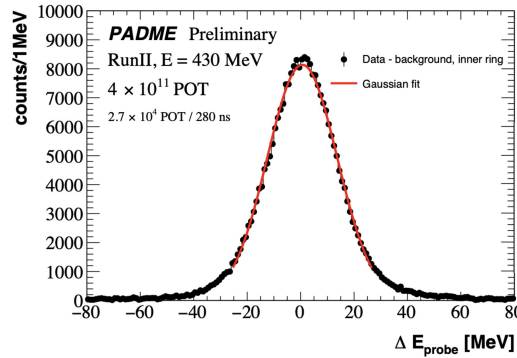


- Below 0.6 GeV known only with 20% accuracy
- Can be sensitive to sub-GeV new physics (e.g. ALPs)
- Using 10% of Run II sample
- Tag-and-probe method on two back-to-back clusters
- Exploit energy-angle correlation

Tag photons selection



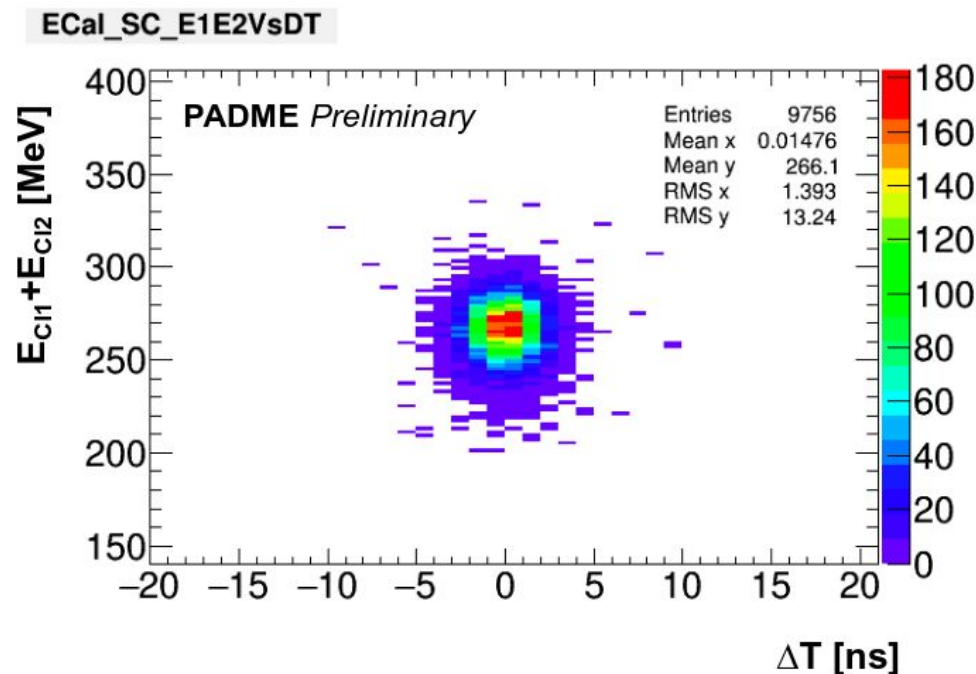
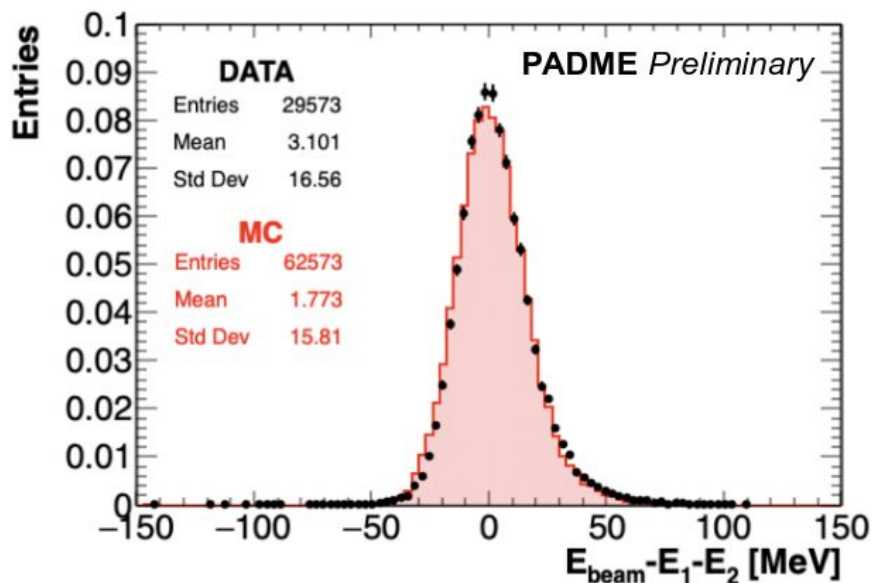
Probe photons



N₂ selection

Events selected \rightarrow N₂(s)

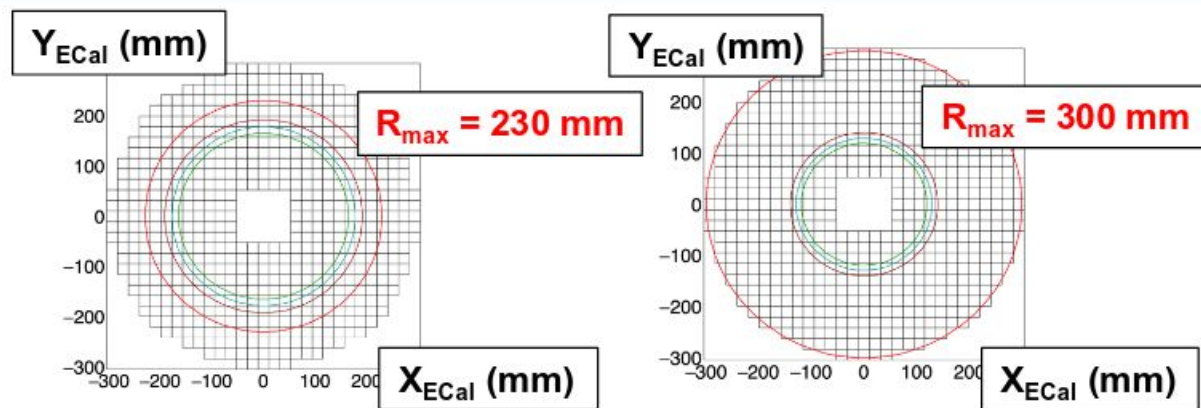
- Events surviving the whole set of cuts, also related to the time difference of the 2 Clusters
- Energy sum of the 2 clusters selected gives back the beam energy (as expected for a two-body final state)
- ECAL relative energy resolution $\sim 5\%$



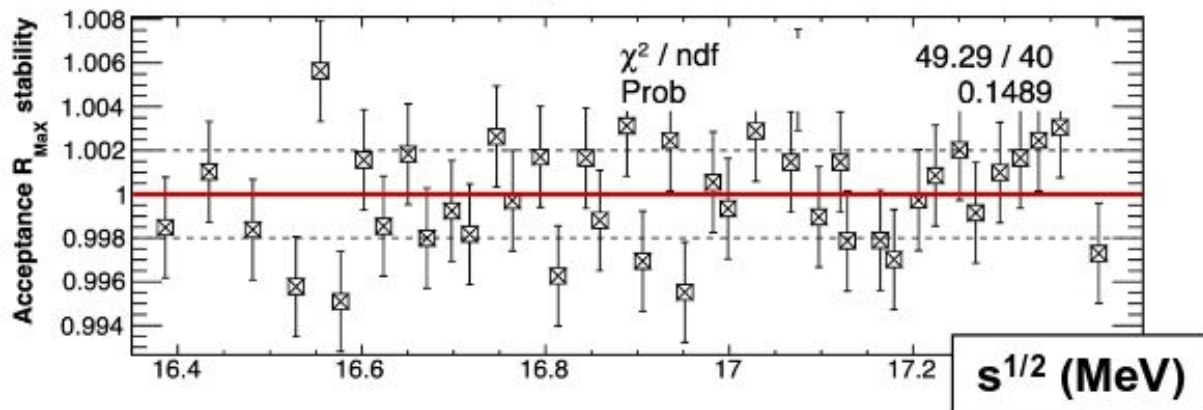
N₂ selection

Stability of R_{max} cuts

- Check if MC and data yields stable vs R_{min}, R_{max} (edge effects, leakage)
- Vary R_{max} by ± 2 ECal cells around nominal cut of 270 mm: 230 mm \rightarrow 300 mm
 - Yield variation: $\sim 10\%$
 - Uncorrelated error 0.3%
- Stability is observed within a coverage band of $\pm 0.2\%$, add 0.035% uncorrelated systematic error on B



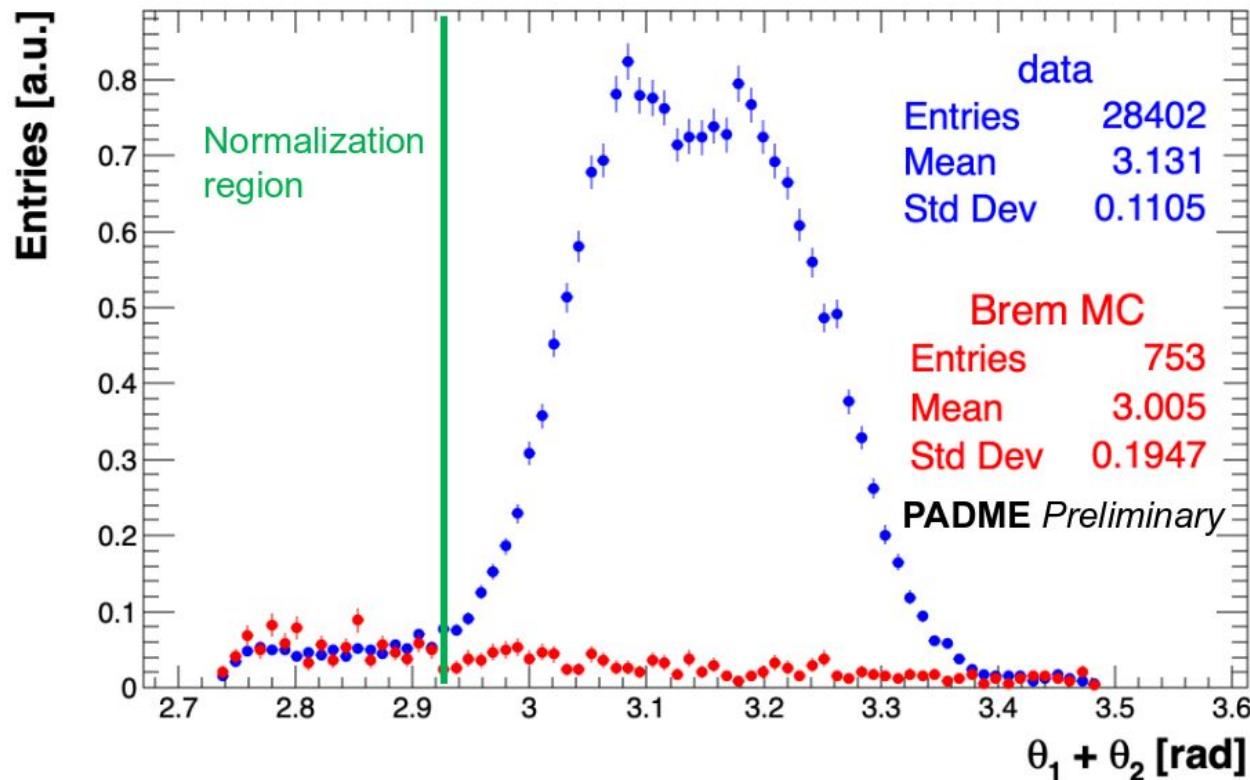
Cut relative stability



N₂ selection

Bremsstrahlung background removal

- In the $\theta_{cm_1} + \theta_{cm_2}$ distribution of the selected event in data and MC shows a Brem tail in outside the signal
- By normalizing in the (0, 2.94 rad) regions and then using the ratio between the (2.94 rad, 4 rad) integrals it is possible to get an estimate of the Brem events under the signal

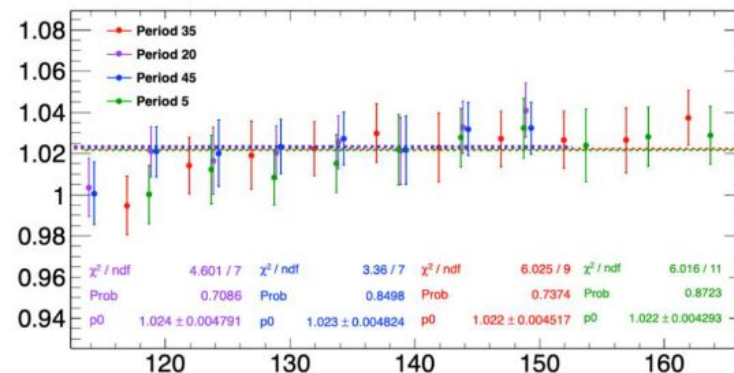


N₂ selection

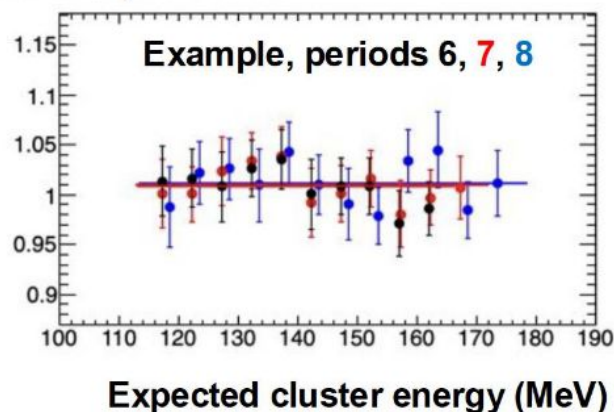
Tag and Probe → Reco efficiency

- Efficiency around 1 within few % except in specific regions (Ecal edges, dead cells)
- Tag & probe: method-induced bias 2.3(2)%, stable along the data set
- Data/MC method efficiency stable along the data set and at the few per mil

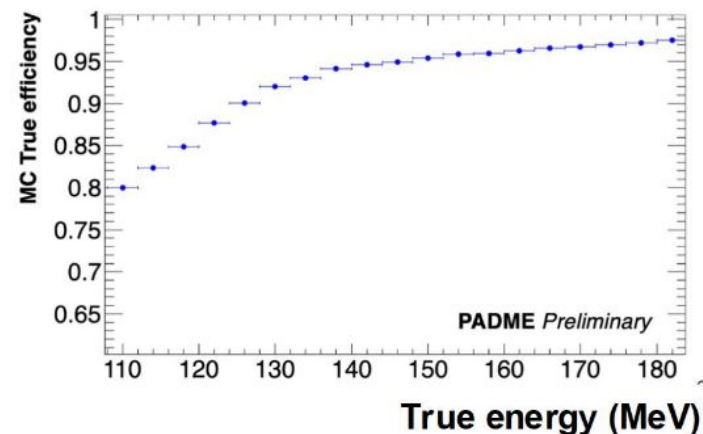
Efficiency <Method /MC true>



Efficiency Data/MC



Expected cluster energy (MeV)



N_{PoT} estimation

PbGI energy loss in passive material

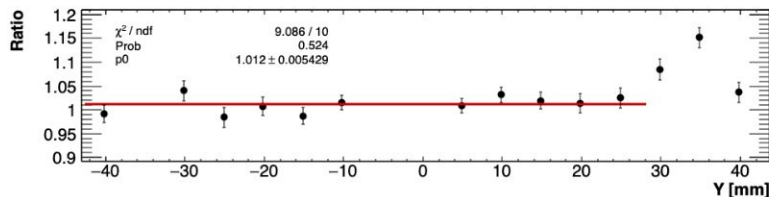
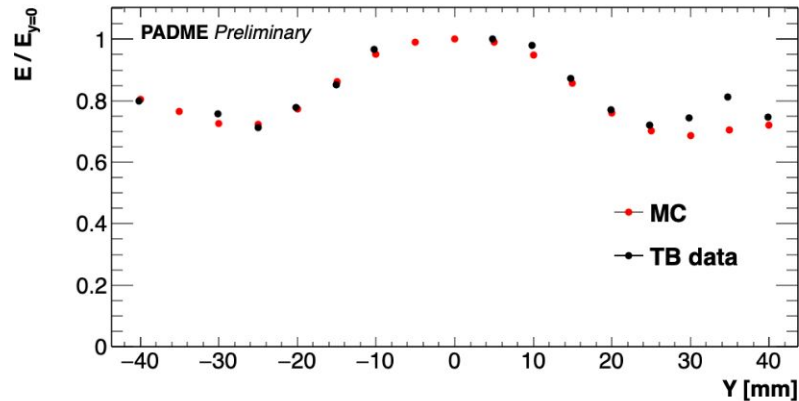
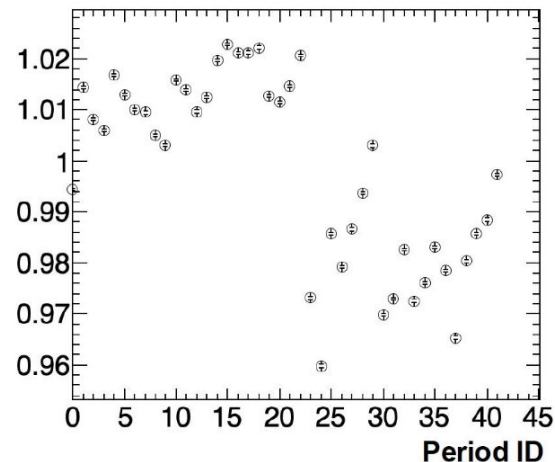
- TimePix cooling geometry (mostly Cu) was described in detail in the MC simulation
- Replicate the loss due to the beam passing in the Cu in Run III is possible by using the beam spot
- Beam spot from TimePix is not available for all the periods → used the COG instead considering the Timepix-ECAL offsets and the intrinsic difference in resolution

Significant period-by-period correction variation: -4% to +2%

How much do we trust the correction?

- Dedicated test beam taking a Y scan at PbGI level. We tried to replicate it with the MC simulation
- Good Data/MC agreement in the region where the beam was scanned during Run III
- 1.2% overall scale correction (included in the $g_R(s)$ scale) with a 0.5% error

Relative leakage correction

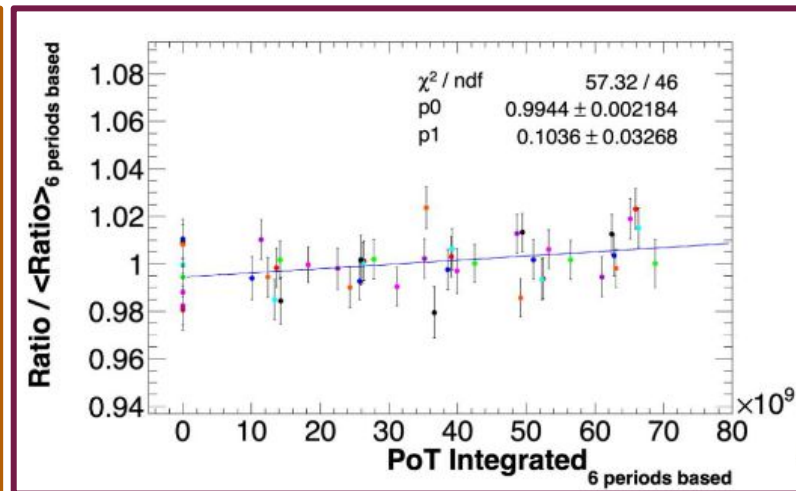
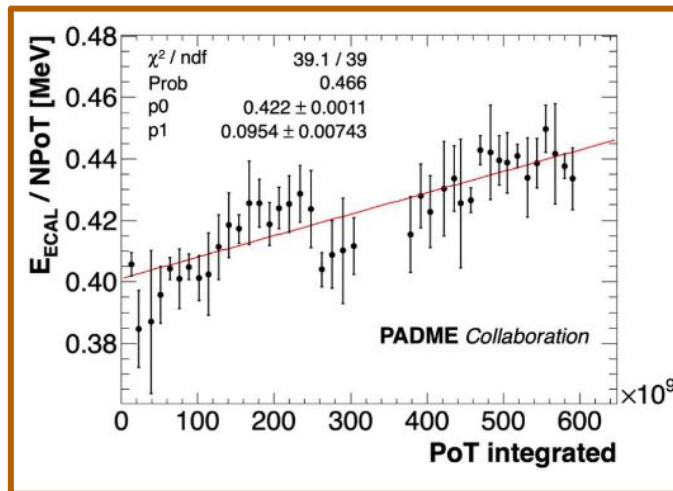
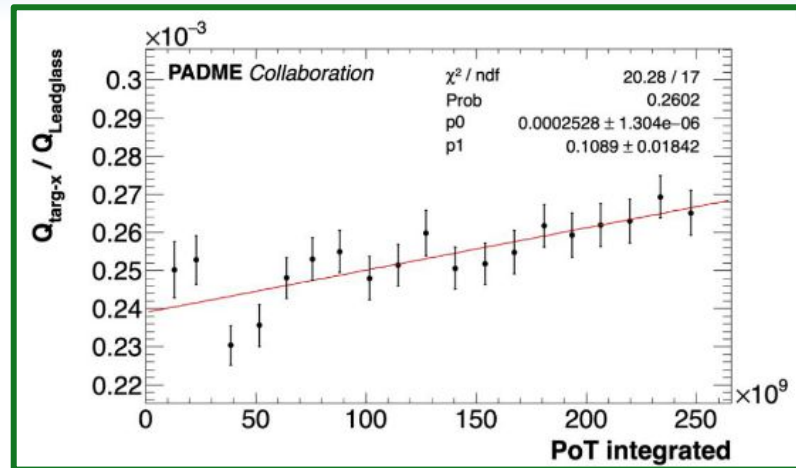


N_{PoT} estimation



Radiation damage

- Throughout Run III a total of $7e11$ PoT (of ~ 300 MeV each) has passed through the PbGI block corresponding to a TID of 25 Gy (2.5 krad)
- The SF57 transmittance loss was never measured in literature, however for similar blocks (SF5-SF6) a significant loss is shown, especially near Cherenkov wavelengths
- Proof of loss of LY:
 - Target X strips are way more sensible than Y \rightarrow their charge can be used for quantitative checks. **10% slope found**
 - The overall energy on ECAL over the NPoT should be a stable quantity, also here we see a **10% slope**
 - Looking at the Data/MC ratio on resetting every 6 periods a compatible slope is found

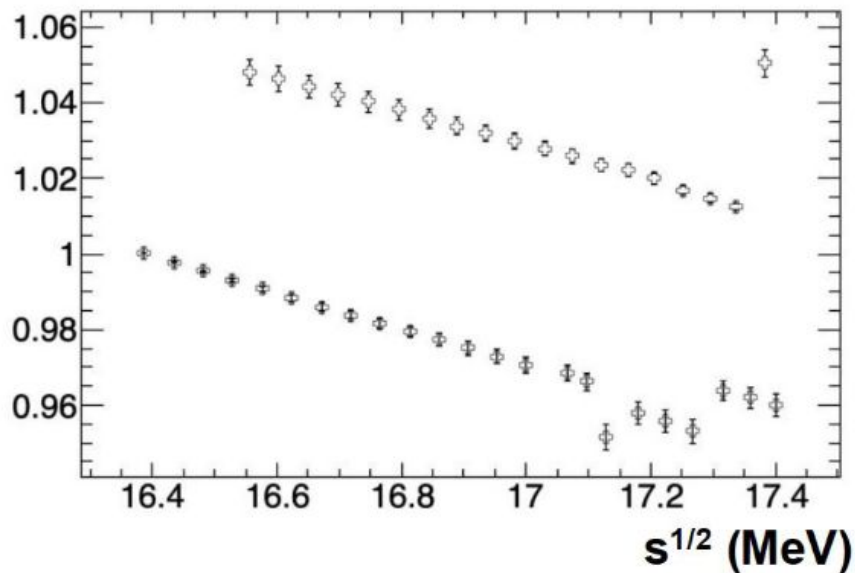


N_{PoT} estimation

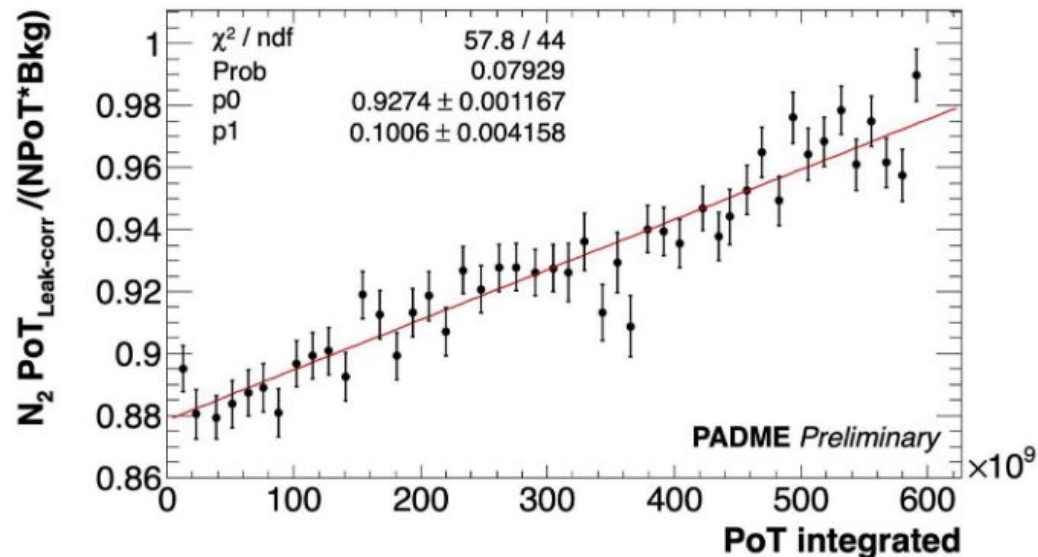
Radiation damage

- PbI yield decreases with relative PoT slope of 0.097(7)
- Constant term uncertainty of 0.3% added as scale error
- Slope error included in PoT uncertainty
- Checked the slope value on $g_R(s)$ after the unblinding \rightarrow totally compatible results

Relative ageing correction



Post unblinding



Unblinding procedure

To validate the error estimate, we applied the procedure in 2503.05650 [hep-ex]

- Aim to blindly define a side-band in $g_R(s)$, excluding 10 periods of the scan
 - Define the masked periods by optimizing the probability of a linear fit in $s^{1/2}$
1. Threshold on the χ^2 fit in side-band is $P(\chi^2) = 20\%$, corresponding to reject 10% of the times
 2. If OK, check if the fit pulls are gaussian
 3. If OK, check if a straight-line fit of the pulls has no slope in $s^{1/2}$ (within 2 sigma)
 4. If OK, check if constant term and slope of the linear fit for $N_2(s)/B(s)$ are within two sigma of the expectations, i.e.: $\pm 4\%$ for the constant, $\pm 2\%$ MeV⁻¹ for the slope

Successfully applied:

1. $P(\chi^2) = 74\%$
2. Pulls gaussian fit probability 60%
3. Slope of pulls consistent with zero
4. Constant term = 1.0116(16), Slope = (-0.010 +- 0.005) MeV⁻¹



Ready to unblind



After box opening, check of the ageing correction applied, slope was 0.097(7)

- Fully consistent (observed excess alters only marginally)
- The slope has been used to correct for the radiation-induced effect, acting as a separate nuisance
- Again no significant change in the location of the excess and in the global p-value

